LARGE DEFORMATION REGISTRATION VIA N-DIMENSIONAL QUASI-CONFORMAL MAPS

YIN TAT LEE, KA CHUN LAM AND LOK MING LUI

Abstract. We propose a new method to obtain registration between n-dimensional manifolds with very large deformations. Given a set of landmark correspondences, our algorithm produces an optimal diffeomorphism that matches prescribed landmark constraints. The obtained registration is a n-dimensional quasi-conformal map. The basic idea of the model is to minimize an energy functional with a conformality term and a smoothness term. The conformality term allows the algorithm to produce diffeomorphisms even with very large deformations. We minimize the energy functional using alternating direction method of multipliers (ADMM). The algorithm only involves solving an elliptic problem and a point-wise minimization problem. The time complexity and robustness of the algorithm is independent of the number of landmark constraints. Either Dirichlet or free boundary condition can be enforced, depending on applications. To further speed up the algorithm, the multi-grid method is applied. Experiments are carried out to test our proposed algorithm to compute landmark-matching registration with different landmark constraints. Results show that our proposed model is efficient to obtain a diffeomorphic registration between n-dimensional data with large deformations.

Key words. Large deformation registration, n-D quasi-conformal, conformality, alternating direction method of multipliers, landmarks

1. Introduction.

Registration refers to the process of finding a meaningful one-to-one pointwise correspondences between different data. The data of interest can be 2D/3D images or geometric shapes. Applications can be found in various fields, such as computer graphics, computer visions and medical imaging. For example, in medical imaging, finding an accurate registration between corresponding anatomical data is necessary for morphometric analysis. While in computer visions, finding accurate 1-1 pointwise correspondences between human faces is crucial for face recognition. Developing effective models for registration is therefore of utmost importance.

Registration can mainly be divided into three categories, namely, the intensity-based registration, landmark-based registration and the hybrid registration. Intensity-based registration aims to obtain good correspondences between data based on the intensity information. For example, the pixel values for image registration and curvatures for surface registration. Landmark-based registration aims to obtain registration based on matching corresponding landmarks. Landmark features can either be manually or automatically labeled. In medical imaging, landmark-based registration is especifically important, since expertise knowledge can be incorporated to label important corresponding features for more accurate and meaningful registration results. One typical example is the brain cortical surface registration for which sulcal landmarks are usually extracted to guide the registration. Hybrid registration combines the intensity-based and landmark-based registration. The registration is guided by both intensity and landmark constraints.

Most existing algorithms work well under small deformations. In some situations, data of interest may undergo large deformations. For instance, cardiac motions of the heart is a large deformation. In these cases, finding a bijective large deformation registration is required. Nevertheless, the computation of large deformation registration is generally challenging. Bijectivity can be easily lost. For the registration between 2D images or surfaces, quasi-conformal theories have been utilized to handle large deformations. The Beltrami coefficient, which measures the conformality distortion, can be effectively used to control the bijectivity of the mapping. By optimizing an energy

functional involving the L^p-norm of the Beltrami coefficient, large deformation diffeomorphic registration can be accurately computed. However, existing quasi-conformal theories apply to 2-dimensional manifolds only. For general n-dimensional spaces, the Beltrami coefficient is not defined. It is our goal in this paper to extend the 2D quasi-conformal theories to general n-dimensional space. In particular, a notion of conformality distortion of a diffeomorphism of the n-dimensional Euclidean space will be formulated. With the definition of conformality distortion, we can extend the 2D quasi-conformal registration algorithm to general n-dimensional manifolds.

In this work, we propose to obtain constrained registration between general n-dimensional spaces by minimizing an energy functional with a conformality term and a smoothness term. The conformality term allows the algorithm to produce diffeomorphisms even with very large deformations. We minimize the energy functional using alternating direction method of multipliers (ADMM). The algorithm only involves solving an elliptic problem and a point-wise minimization problem. The time complexity and robustness of the algorithm is independent of the number of landmark constraints. Either Dirichlet or free boundary condition can be enforced, depending on applications. To further speed up the algorithm, the multi-grid method is applied. We test the proposed algorithm to compute landmark-matching registration with different landmark constraints. Experimental results show that our proposed algorithm is effective for computing large deformation diffeomorphic registrations, even with large number of landmarks or large deformations.

The paper is organized as follows. In Section 2, some previous works closely related to our paper will be reviewed. Basic mathematical background will be explained in Section 3. In Section 4, we describe our proposed model to obtain the constrained large deformation registration between n-dimensional manifolds in details. The numerical algorithm will be discussed in Section 5. Experimental results will be demonstrated in Section 6. Conclusion and future works will be discussed in Section 7.

2. Previous works. In this section, we will review some related works closely related to this paper.

Intensity-based image registration has been widely studied [1]. One commonly used approach is done by minimizing an energy functional involving the intensity mismatching error. Vercauteren et al. [24] proposed the diffeomorphic demons registration algorithm, which is based on Thirion's demons algorithm[3]. The obtained registration is guaranteed to be diffeomorphic by adapting the optimization procedure underlying the demons algorithm to a space of diffeomorphic transformations. Glocker et al. [40][41][42] proposed the intensity-matching image registration algorithm using the Markov random field. Surface registration that matches geometric quantities, such as curvatures, have also been extensively studied [4][2][23][25]. Lyttelton et al. [2] proposed an algorithm for surface parameterizations based on matching surface curvatures. Yeo et al. [25] proposed the spherical demons method, which adopted the diffeomorphic demons algorithm [24], to drive surfaces into correspondence based on the mean curvature and average convexity. Conformal surface registration, which minimizes angular distortions, has also been widely used to obtain a smooth 1-1 correspondence between surfaces [13, 5, 7, 6, 14, 15, 16, 17]. Besides, quasi-conformal surface registrations, which allows bounded amount of conformality distortion, have also been studied [18, 19, 20, 21]. For example, Lui et al. [19] proposed to compute quasi-conformal registration between hippocampal surfaces based on the holomorphic Beltrami flow method, which matches geometric quantities (such as curvatures) and

minimizes the conformality distortion [18].

Landmark-based registration has also been widely studied. Bookstein et al. [26] proposed to apply a thin-plate spline regularization (or biharmonic regularization) to obtain a registration with soft landmark constraints. Tosun et al. [31] proposed to combine iterative closest point registration, parametric relaxation and inverse stereographic projection to align cortical sulci across brain surfaces. These diffeomorphisms obtained can better match landmark features, although not perfectly. Wang et al. [27, 30, 28, 29] proposed to compute the optimized harmonic registrations of brain cortical surfaces by minimizing a compounded energy involving the landmark-mismatching term [27, 30]. The obtained registration obtains an optimized harmonic map that better aligns the landmarks. However, landmarks cannot be perfectly matched, and bijectivity cannot be guaranteed under large number of landmark constraints. Again, landmarks cannot be exactly matched. In the situation when exact landmark matching is required, smooth vector field has been used. Lui et al. [28, 29] proposed the use of vector fields to represent surface maps and reconstruct them through integral flow equations. They obtained shape-based landmark matching harmonic maps by looking for the best vector fields minimizing a shape energy. The use of vector fields to compute the registration makes the optimization easier, although it cannot describe all surface maps. An advantage of this method is that exact landmark matching can be guaranteed. Time dependent vector fields can also be used [8, 9, 10, 11, 12]. For example, Glaunés et al. [9] proposed to generate large deformation diffeomorphisms of a sphere, with given displacements of a finite set of template landmarks. The time dependent vector fields facilitate the optimization procedure, although it may not be a good representation of surface maps since it requires more memory. The computational cost of the algorithm is also expensive. Quasi-conformal mapping that matches landmarks consistently has also been proposed. Wei et al. [34] also proposed to compute quasi-conformal mappings for feature matching face registration. However, either exact landmark matching or the bijectivity of the mapping cannot be guaranteed, especially when very large deformations occur.

Algorithms for hybrid registration, which combines both the landmark and intensity information to guide the registration, has also been proposed[36][37][35][38][43]. For example, Christensen et al. [38] propsoed an algorithm for hybrid registration that uses both landmark and intensity information to guide the registration. The method utilizes the unidirectional landmark thin-plate spline (UL-TPS) registration technique together with a minimization scheme for the intensity difference to obtain good correspondence between images. Paquin et al. [36] proposed a registration method using a hybrid combination of coarse-scale landmark and B-splines deformable registration techniques.

3. Mathematical background. In this section, we describe some basic mathematical concepts related to our algorithms. For details, we refer the readers to [32][33].

A surface S with a conformal structure is called a *Riemann surface*. Given two Riemann surfaces M and N, a map $f : M \to N$ is *conformal* if it preserves the surface metric up to a multiplicative factor called the conformal factor. An immediate consequence is that every conformal map preserves angles. With the angle-preserving property, a conformal map effectively preserves the local geometry of the surface structure.

A generalization of conformal maps is the *quasi-conformal* maps, which are orientation preserving homeomorphisms between Riemann surfaces with bounded confor-

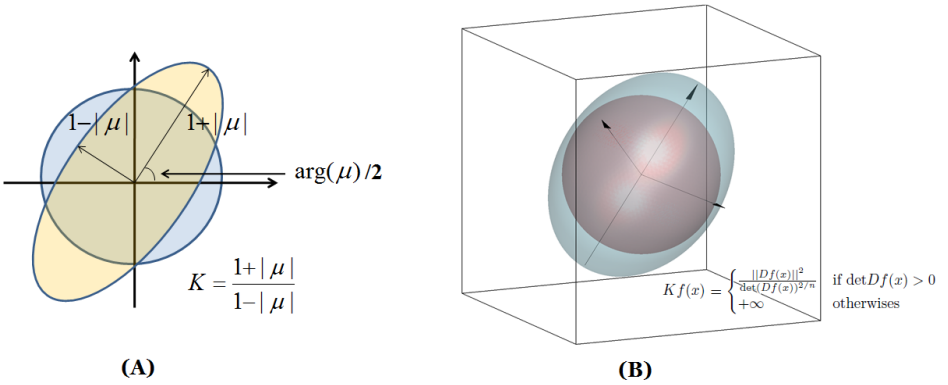

FIG. 3.1. *Illustration of the conformality distortion. (A) shows the how a small circle is deformed to an ellipse under a 2D quasi-conformal map. The conformality distortion is measured by the Beltrami coefficient. (B) shows how a small ball is deformed to a small ellipsoid under a 3D diffeomorphism. The conformality distortion can be measured by $K(f)$ defined in this paper.*

mality distortion, in the sense that their first order approximations takes small circles to small ellipses of bounded eccentricity [32]. Thus, a conformal homeomorphism that maps a small circle to a small circle can also be regarded as quasi-conformal. Surface registrations and parameterizations can be considered as quasi-conformal maps. Mathematically, $f : \mathbb{C} \to \mathbb{C}$ is quasi-conformal provided that it satisfies the Beltrami equation:

$$\frac{\partial f}{\partial \overline{z}} = \mu(z)\frac{\partial f}{\partial z}. \tag{3.1}$$

for some complex valued Lebesgue measurable μ satisfying $||\mu||_\infty < 1$. μ is called the *Beltrami coefficient*, which is a measure of non-conformality. In particular, the map f is conformal around a small neighborhood of p when $\mu(p) = 0$. Infinitesimally, around a point p, f may be expressed with respect to its local parameter as follows:

$$\begin{aligned} f(z) &= f(p) + f_z(p)z + f_{\overline{z}}(p)\overline{z} \\ &= f(p) + f_z(p)(z + \mu(p)\overline{z}). \end{aligned} \tag{3.2}$$

Obviously, f is not conformal if and only if $\mu(p) \neq 0$. Inside the local parameter domain, f may be considered as a map composed of a translation to $f(p)$ together with a stretch map $S(z) = z + \mu(p)\overline{z}$, which is postcomposed by a multiplication of $f_z(p)$, which is conformal. All the conformal distortion of $S(z)$ is caused by $\mu(p)$. $S(z)$ is the map that causes f to map a small circle to a small ellipse. From $\mu(p)$, we can determine the angles of the directions of maximal magnification and shrinking and the amount of them as well. Specifically, the angle of maximal magnification is $\arg(\mu(p))/2$ with magnifying factor $1 + |\mu(p)|$; The angle of maximal shrinking is the orthogonal angle $(\arg(\mu(p)) - \pi)/2$ with shrinking factor $1 - |\mu(p)|$. The distortion or dilation is given by:

$$K = 1 + |\mu(p)|/1 - |\mu(p)|. \tag{3.3}$$

Thus, the Beltrami coefficient μ gives us all the information about the properties of the map (See Figure 3.1(A)).

Given a Beltrami coefficient $\mu : \mathbb{C} \to \mathbb{C}$ with $\|\mu\|_\infty < 1$. There is always a quasiconformal mapping from $\mathbb{C}$ onto itself which satisfies the Beltrami equation in the distribution sense [32].

However, the above quasi-conformal theories only apply to two dimensional spaces or surfaces. In this work, our goal is to extend the idea of 2-dimensional quasi-conformal theories to general n-dimensional spaces. We will introduce a notion of conformality distortion of a diffeomorphism of the n-dimensional space. The conformality distortion measures the distortion of an infinitesimal ball to an infinitesimal ellipsoid under the diffeomorphism (See Figure 3.1(B)).

4. Proposed model. In this section, we will explain in details our proposed model to obtain the constrained large deformation registration between n-dimensional manifolds. The basic idea is to formulate the notion of conformality distortion of a diffeomorphism of the n-dimensional Euclidean space. The conformality distortion measures the distortion of an infinitesimal ball to an infinitesimal ellipsoid under the diffeomorphism. The constrained registration problem can then be modeled as minimizing an energy functional involving the conformality term and the smoothness term. We first present the continuous model of the proposed energy functional. Then, we explain the discretization of the model.

4.1. The continuous model. Let $\Omega \subset \mathbb{R}^n$ be the domain of image. Let $f : \Omega \to \Omega$ be the transformation. For $x \in \Omega$, define $T_x\Omega$ to be the set of tangent vectors at x. The mapping f define a mapping df from $T_x\Omega$ to $T_{f(x)}\Omega$ by the formula $df_x(v) = Df(x)v$ where $Df(x)$ is the Jacobian matrix of f at point x. Let E_x the set of v such that $||df_x(v)|| = 1$. These v must satisfy $v^t Df(x)^t Df(x)v = 1$. Since $Df(x)^t Df(x)$ is a non-negative symmetric matrix, E_x is an ellipse. Geometrically, E_x is an infinitesimally small ellipse around x, which maps to an infinitesimally small circle at $f(x)$. Therefore, it reveals the distortion of the mapping f at point x (See 3.1(B)). In landmark registration problem, it is favorable to have a smooth mapping with small distortions.

Let us first define the distance between an ellipsoid $E = \{x : x^t Ax = 1\}$ and a ball where A is some positive symmetric matrix. Since the distance should be invariant under rotation, we assume A is diagonal matrix $diag(\lambda_1, \cdots \lambda_n)$. Notice that $(\lambda_1 \cdots \lambda_n)^{1/n} \leq \frac{\lambda_1 + \cdots + \lambda_n}{n}$ where the equality sign holds if and only if $\lambda_1 = \cdots = \lambda_n$. The ratio between two sides measures the distance between E and a circle. Therefore, we define the distortion of the mapping f at point x by

$$\begin{aligned} Kf(x) &= \begin{cases} \frac{\mathrm{tr}(Df(x)^t Df(x))}{\det(Df(x))^{2/n}} & \text{if } \det Df(x) > 0 \\ +\infty & \text{otherwises} \end{cases} \\ &= \begin{cases} \frac{||Df(x)||^2}{\det(Df(x))^{2/n}} & \text{if } \det Df(x) > 0 \\ +\infty & \text{otherwises} \end{cases}. \end{aligned}$$

Also, we have $Kf(x) \geq n$ and $Kf(x) = n$ if and only if E_x is a ball. Therefore, $Kf(x)$ attains the minimum when f is conformal at point x. $Kf(x)$ is called the *conformality distortion* of the map f.

In 2-dimensional case,

$$Kf(x) = 2\frac{1 + |\mu(x)|^2}{1 - |\mu(x)|^2}$$

where $\mu(x)$ is the Beltrami coefficient. Therefore, if $||Kf(x)||_\infty < K$, the mapping is K'-quasiconformal mapping (with certain constant $K' > 1$ depending on K). In our model, our goal is to make $||Kf(x)||_\infty < K$ for certain $K < \infty$. As a result, the model produce diffeomorphisms even for large deformation problems. We minimize $||Kf(x)||_1$ for performance consideration. In the discrete case, it can still guarantee the diffeomorphism.

With the notion of conformality distortion, we propose to obtain an optimal diffeomorphism that satisfies the landmark constraints by minimizing an energy functional. Experimental results shows that the minimizer of the $\int Kf(x)$ only can be piecewise linear. In order to enhance the smoothness of the mapping, we consider the following minimization problem:

$$\inf_{f \in F} \int Kf(x) + \frac{\sigma}{2} ||\nabla^2 f(x)||^2 dx \tag{4.1}$$

where $\sigma > 0$ is fixed parameter and F is the set of function $f : \Omega \to \mathbb{R}^n$ which is surjective and satisfies the landmark constraint $f(p_i) = q_i$ for p_i and q_i are given landmark points $(i = 1, 2, ..., m)$.

4.2. The discrete model. For general manifold, our model (4.1) can be discretized by using discrete differential forms. Since our experiments are performed on a cubic domain, we only explain the discretization of (4.1) on a cubic domain here. First, we pick a tetrahedral mesh for the cubic domain such that each tetrahedron in the mesh contains 3 edges, each one of them is parallel to the one of the three coordinate axis respectively. In our implementation, we partition the cubic domain into small equal-size cubes and create similar tetrahedral meshes for each cubes. For the unit cube with vertices

$$\{(0,0,0),(0,0,1),(0,1,0),(1,0,0),\cdots,(1,1,1)\},$$

we use the tetrahedral mesh with 6 tetrahedrons. The vertices for that 6 tetrahedrons are

$$\begin{gathered}\{(0,0,0),(1,0,0),(0,0,1),(1,1,0)\},\\ \{(0,0,0),(0,1,0),(0,0,1),(1,1,0)\},\\ \{(0,0,1),(0,1,0),(0,1,1),(1,1,0)\},\\ \{(1,0,0),(0,0,1),(1,1,0),(1,0,1)\},\\ \{(0,0,1),(1,1,0),(1,0,1),(1,1,1)\},\\ \{(0,0,1),(0,1,1),(1,1,0),(1,1,1)\}.\end{gathered}$$

Since each tetrahedron contains 3 edges parallel to the 3-axises respectively, for each piecewise linear f defined on the tetrahedrons, $D_x f$, $D_y f$ and $D_z f$ can be computed by finite difference directly. Denote $Df(T)$ is a 3×3 Jacobian matrix for each tetrahedron T.

The discrete version of (4.1) is given by

$$\inf_{f \in F} \sum_{\text{tetrahedron } T} Kf(T) + \frac{\sigma}{2} \sum_{\text{node } x} ||\Delta f(x)||^2$$

where F is the set of function defined on nodes of the mesh, seven-point Laplacian stencil with suitable boundary condition is used for Δf and $Kf(T)$ is defined by:

$$Kf(T) = \begin{cases} \frac{||Df(T)||^2}{\det(Df(T))^{2/n}} & \text{if } \det Df(T) > 0 \\ +\infty & \text{otherwises} \end{cases}.$$

5. Algorithm. In this section, we explain the numerical algorithm to optimize the energy functional described in the last section. We apply the alternating direction method of multipliers (ADMM) to minimize the energy. Since the term $Kf(T)$ is $+\infty$ when $\det Df(T) \leq 0$, the algorithm should avoid this case. However, finding a mapping such that $\det Df(T) > 0$ and $f(p_i) = q_i$ is a non-trivial task itself. To avoid this difficulty, we use the alternating minimization scheme to split the problem as follows:

$$\inf_{f \in F} \sum_{\text{tetrahedron } T} K(f, R, T) + \frac{\sigma}{2} \sum_{\text{node } x} ||\Delta f(x)||^2 \quad \text{given } R(T) = Df(T)$$

where:

$$K(f, R, T) = \begin{cases} \frac{||Df(T)||^2}{\det(R(T))^{2/3}} & \text{if } \det R(T) > 0 \\ +\infty & \text{otherwises} \end{cases}.$$

More explicitly, we have the following algorithm:

Algorithm 1: Constrained quasi-conformal registration

1. $f^1 =$ identity map, $\lambda^1 = 0, R^1 = Df^1$.
2. While $||f^{k+1} - f^k|| > \varepsilon$
3. Find $f^{k+1} = \underset{f}{\operatorname{argmin}} \sum_T K(f, R, T) + \frac{\mu}{2} \sum_T ||R(T) - Df(T) + \lambda^k(T)||^2 + \frac{\sigma}{2} \sum_x ||\Delta f(x)||^2$.
4. Find $r^{k+1}(T) = \underset{\det R > 0}{\operatorname{argmin}} K(f, R, T) + \frac{\mu}{2} ||R - Df(T) + \lambda^k(T)||^2$ for each tetrahedron T.
5. $\lambda^{k+1} = \lambda^k + R(T) - Df(T)$.
6. End While

There are two subproblem, which are step 3 and step 4, in the algorithm. We do the f-subproblem first because it gives good approximation of the mapping even if the approximations of R^1 and λ^1 are bad. Hence, it avoid the algorithm from getting stuck at a local minimum. In the following two subsections, we will explain step 3 and step 4 in details.

5.1. f-subproblem. The f-subproblem is to minimize the energy

$$\sum_T \frac{||Df(T)||^2}{\det(R(T))^{2/3}} + \frac{\mu}{2} \sum_T ||R(T) - Df(T) + \lambda^k(T)||^2 + \frac{\sigma}{2} \sum_x ||\Delta f(x)||^2.$$

We remark that $f = (f_1, f_2, f_3)$ is a vector. Since the equation for f_i is decoupled, we can solve it component-wise. Therefore, we can regard f as a scalar function only in this section. The corresponding Euler-Lagrange equation for this problem is of the form

$$\begin{cases} \Delta^2 f(x) - \nabla \cdot (A(x)\nabla f(x)) &= g(x); \\ f(p_i) &= q_i, \end{cases} \tag{5.1}$$

where $A(x)$ is a diagonal matrix depends on $\det(R(T))^{2/3}$ and $g(x)$ depends on $R(T)+\lambda^k(T)$. By subtracting f by $f(p_i) = q_i$, we can assume $f(p_i) = 0$.

The diagonal entries of $A(x)$ is of the form

$$\sum_{\text{six } T \text{ touch the corresonding edge}} \frac{1}{\sigma}\left(\frac{1}{\det(R(T))^{2/3}} + \mu\right).$$

In our actual implementation, we choose $\mu \sim \max \frac{30}{\det(R(T))^{2/3}}$ and the equation can be approximate by

$$\begin{cases} \Delta^2 f(x) - \frac{6\mu}{\sigma}\Delta f(x) &= g(x); \\ f(p_i) &= 0, \end{cases} \tag{5.2}$$

Therefore, we could solve the equation (5.1) using preconditioned conjugate gradients squared method where the preconditioner is a multigrid vcycle for the equation (5.2). The equation (5.2) can be splitted into two coupled Poisson equations

$$\begin{cases} -h - \Delta f &= 0; \\ -\Delta h - \Delta_A f &= g; \\ f(p_i) &= 0, \end{cases} \tag{5.3}$$

where $\Delta_A = \nabla \cdot (A(x)\nabla f(x))$. The boundary condition on a face of both equation is Dirichlet when the face of that component is fixed and is Neumann otherwise. For the restriction and interpolation operator, full weighting restriction and bilinear interpolation operator are used. On the coarse grid, the landmark point p_i^{coarse} are chosen to be the set of all points on coarse code that is nearest to p_i. Therefore, for each p_i, there is either 1, 2, 4 or 8 corresponding p_i^{coarse}. This choice of p_i^{coarse} makes the interpolated function from coarse grid satisfies the landmark condition $f(p_i) = 0$ automatically. For the pre and post smoothing operator, four steps Red-Black Gauss Seidel is used where on each point the corresponding 2×2 matrix is solved directly. Although the vcycle itself may not converges because of the landmark condition, the experimental results show that it is a very good preconditioner.

5.2. R-subproblem. The minimization problem is a tetrahedron-wise problem. The Euler Lagrange equation for this problem is

$$R - \frac{a}{(\det R)^{2/3}}(R^{-1})^t = B \tag{5.4}$$

where $a = \frac{2||Df(T)||^2}{3\mu}$ and $B = Df(T) - \lambda^k(T)$. The equation above can be simplified by SVD. Let the SVD of B is $U\Sigma V^*$. Then the equation reduced to system of equations with three variables:

$$\tilde{\Sigma} - \frac{a}{\left(\det\tilde{\Sigma}\right)^{2/3}}\tilde{\Sigma}^{-1} = \Sigma$$

where the SVD of R is $U\tilde{\Sigma}V^*$. Since the system is coupled by the term $\det\tilde{\Sigma}$, we can solve the equation iteratively by

$$\tilde{\Sigma}_n - \frac{a}{\left(\det\tilde{\Sigma}_{n-1}\right)^{2/3}}\tilde{\Sigma}_n^{-1} = \Sigma$$

where $\tilde{\Sigma}_n$ is the $\tilde{\Sigma}$ in step n. Now, it can be solved by quadratic formula. Note that there are two possible solutions for quadratic formula and hence the solution for the equation (5.4) is not unqiue. Since $R \sim Df$. we want R to be close to be postive symmetric definite. When $\det B > 0$, we choose both three eigenvalues of $\tilde{\sum}$ to be positive, otherwises, we choose the smallest eigenvalue to be negative. To sum up, we solve this problem by the following iterative scheme:

Algorithm 2: Solving (5.4)

1. Compute the SVD of $B = U\Sigma V^*$ where the diagonal of Σ is x_i.
2. $d^1 = (\det R^{(\text{last})})^{2/3}$
3. While $||d^{k+1} - d^k|| > \varepsilon$
4. Compute $y_i^k = \frac{1}{2}(x_i + \sqrt{x_i^2 + \frac{4a}{d^k}})$ for $i = 1, 2, 3$.
5. If $\det B < 0$, Compute $y_i^k = \frac{1}{2}(x_i - \sqrt{x_i^2 + \frac{4a}{d^k}})$ for $i = \text{argmin}_i x_i$.
6. Compute $d^{k+1} = \frac{1}{2}\text{sgn}(\det B)\left(d^k + \left(y_1^k y_2^k y_3^k\right)^{2/3}\right)$.
7. End While
8. $R = U\tilde{\Sigma}V^*$ where diagonal of $\tilde{\Sigma}$ is y_i.

Theorem 5.1. *Given any 3×3 matrix B, $a > 0$. The algorithm 2 converges linearly with the rate $\frac{1}{2}$ to the global minimizer of*

$$\min_{detR>0} \frac{a}{\frac{2}{3}\det(R)^{2/3}} + \frac{1}{2}||R - B||^2.$$

Proof. Let the SVD of B is $U\Sigma V^*$. Then SVD of H is $U\tilde{\Sigma}V^*$ where $\tilde{\Sigma}$ is a diagonal matrix satisfies the equation

$$\tilde{\Sigma} - \frac{a}{\left(\det\tilde{\Sigma}\right)^{2/3}}\tilde{\Sigma}^{-1} = \Sigma.$$

Let the diagonal of Σ is x_i and the diagonal of $\tilde{\Sigma}$ is y_i, we have $y_i - \frac{a}{D}y_i^{-1} = x_i$ where $D = \text{sgn}(\det B)(y_1y_2y_3)^{2/3}$. Solving the quadratic equation, we have

$$y_i(D) = \frac{x_i \pm \sqrt{x_i^2 + \frac{4a}{D}}}{2} \tag{5.5}$$

where the sign is chosen according to the algorithm. Since we want to minimize the following energy

$$\frac{a}{\frac{2}{3}\det(R)^{2/3}} + \frac{1}{2}||R - B||^2 = \frac{3a}{2(y_1y_2y_3)^{2/3}} + \frac{1}{2}\sum\left(x_i - y_i\right)^2,$$

we want to make D larger and y_i closer to x_i. Therefore, it is direct but tedious to verify that: If $\det B > 0$, then the minimizer satisfies the + sign in the (5.5) for all i.

If $\det B < 0$, the minimizer satisfies the + sign in the (5.5) for all $i \neq \text{argmin}_i x_i$. This explains the purpose of step 5. Without loss of generality, assume $\text{argmin}_i x_i = 1$.

Let $F(D) = (y_1(D)y_2(D)y_3(D))^{2/3}$ and $G(D) = \frac{D+F(D)}{2}$. We have

$$F'(D) = \frac{-2a}{3D^2} F(D) \sum_{i=1}^{3} \frac{\pm 1}{y_i} \frac{1}{\sqrt{x_i^2 + \frac{4a}{D}}}$$

where the $\pm$ sign is the sign chosen in y_i. Note that each term $\frac{\pm 1}{y_i} \frac{1}{\sqrt{x_i^2+\frac{4a}{D}}}$ in that sum is positive. Hence $F'(D) \leq 0$.

For the case $\det D > 0$, we have

$$\begin{aligned} -F'(D) &= \frac{2a}{3D^2} F(D) \sum_{i=1}^{3} \frac{1}{y_i} \frac{1}{\sqrt{x_i^2 + \frac{4a}{D}}} \\ &< \frac{2a}{3D^2} F(D) \sum_{i=1}^{3} \frac{D}{2a} \\ &= \frac{F(D)}{D}. \end{aligned}$$

For the case $\det D < 0$, we have

$$\begin{aligned} \frac{-1}{y_1 \sqrt{x_1^2 + \frac{4a}{D}}} &= \frac{2}{\sqrt{x_1^2 + \frac{4a}{D}} - x_1^2} \frac{1}{\sqrt{x_1^2 + \frac{4a}{D}}} \\ &= \frac{D}{2a} \frac{x_1 + \sqrt{x_1^2 + \frac{4a}{D}}}{\sqrt{x_1^2 + \frac{4a}{D}}}. \end{aligned}$$

On the other hand, for $i = 2, 3$, we have

$$\begin{aligned} \frac{1}{y_i \sqrt{x_i^2 + \frac{4a}{D}}} &= \frac{2}{x_i^2 + \frac{4a}{D}} \frac{\sqrt{x_i^2 + \frac{4a}{D}}}{x_i + \sqrt{x_i^2 + \frac{4a}{D}}} \\ &\leq \frac{D}{2a} \frac{\sqrt{x_1^2 + \frac{4a}{D}}}{x_1 + \sqrt{x_1^2 + \frac{4a}{D}}} \end{aligned}$$

because the last term is decreasing function. Hence we have

$$-F'(D) \leq \frac{2a}{3D^2} F(D) \frac{D}{2a} \left(\frac{x_1 + \sqrt{x_1^2 + \frac{4a}{D}}}{\sqrt{x_1^2 + \frac{4a}{D}}} + 2 \frac{\sqrt{x_1^2 + \frac{4a}{D}}}{x_1 + \sqrt{x_1^2 + \frac{4a}{D}}} \right).$$

Since $\frac{1}{2} < \frac{\sqrt{x_1^2+\frac{4a}{D}}}{x_1+\sqrt{x_1^2+\frac{4a}{D}}} < 1$, the last term is less then 3.

Hence, we have $-F'(D) \leq \frac{F(D)}{D}$.

Let $\tilde{D}$ be the solution of $G(D) = D$. For the case $D \geq \tilde{D}$, we have

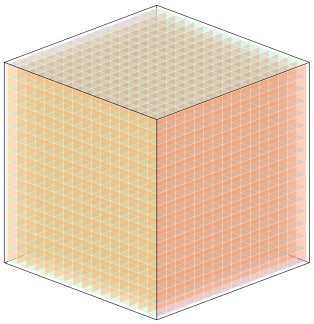

FIG. 6.1. *A regular grid of a cube discretizing the source domain.*

$$\frac{1}{2} > G'(D) > \frac{1}{2} - \frac{F(D)}{D} > 0.$$

Hence $\frac{D+\tilde{D}}{2} > G(D) > \tilde{D}$. For the case $D \leq \tilde{D}$, we have $G(D) = \frac{D+F(D)}{2} > \frac{D+\tilde{D}}{2}$. If $G^{\circ n}(D) > \tilde{D}$ for some n, then it keeps larger than $\tilde{D}$ and converges to $\tilde{D}$ with rate $\frac{1}{2}$. Otherwise, it also converges to $\tilde{D}$ with rate $\frac{1}{2}$. □

6. Experimental Result. In this section, we show some experimental results. We test our proposed algorithm to compute constrained 3-dimensional quasi-conformal registrations with different landmark constraints.

We first test our algorithm to compute constrained registration with one landmark. Figure 6.2(A) shows how the landmark point is deformed. The deformation of the landmark point is large. Using the proposed algorithm, we obtain a diffeomorphic registration that satisfies the landmark constraint exactly. Figure 6.2(B) shows the registration result. It is visualized as the deformation of the original reference mesh as shown in Figure 6.1 under the obtained registration. The reference mesh is a regular grid of a cube discretizing the source domain. Our obtained landmark-matching registration is diffeomorphic. Figure 6.2(C) shows the visualization of the obtained registration with a sparser view (to better demonstrate the registration result).

Secondly, we test the algorithm to compute the constrained registration with an inner sphere being chosen as landmarks. In other words, points of an inner sphere are chosen as landmarks and they are rotated anti-clockwisely, as shown in Figure 6.3(A). The obtained registration, which is visualized as the deformation of the standard grid by the registration, is shown in Figure 6.3(B). Figure 6.3(C) visualizes the obtained registration with a sparser view. Note that the obtained registration is diffeomorphic, even with a large number of landmarks and large deformations.

Next, we test the algorithm on an example of which all the points on a plane are chosen as landmarks (grey plane in Figure 6.4(A)). The landmarks are deformed to a wave-shape surface (red surface in Figure 6.4(A)). Using our proposed algorithm, we obtain a 3-dimensional quasi-conformal map that satisfies the landmark constraints. Figure 6.4(B) shows the obtained registration, which is diffeomorphic. Figure 6.4(C) shows the registration with a sparser view.

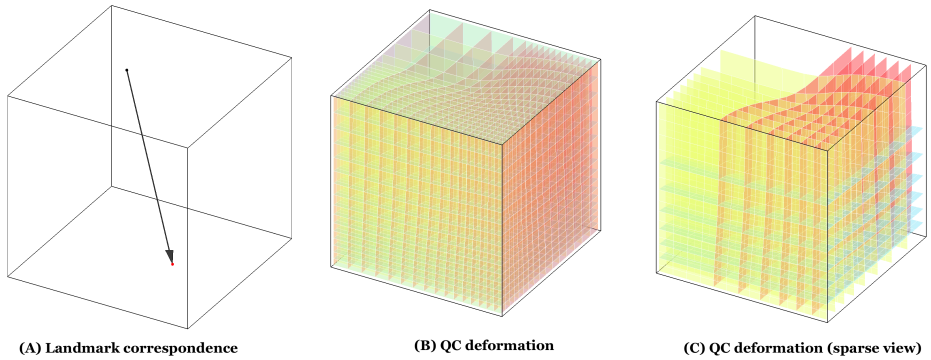

FIG. 6.2. *One point landmark matching registration. (A) shows the landmark correspondence of one point. (B) shows the obtained constrained QC registration, which is visualized as the deformed grid from the standard grid in Figure 6.1 by the obtained registration. (C) shows the sparser view of the registration.*

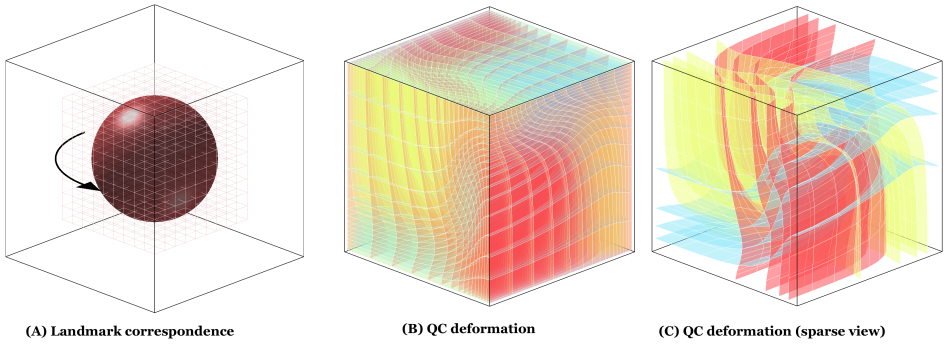

FIG. 6.3. *Constrained registration with an inner sphere being chosen as landmarks. Landmarks are rotated anti-clockwisely by 90 degrees. (A) shows the landmark correspondence of one point. (B) shows the obtained constrained QC registration, which is visualized as the deformed grid from the standard grid in Figure 6.1 by the obtained registration. (C) shows the sparser view of the registration.*

Finally, we test the algorithm to compute a constrained registration with random points being chosen as landmarks. These random landmark points are twisted, as shown in Figure 6.5(A). The twist deformation is quite large. Using our algorithm, we are able to obtain a diffeomorphic landmark-matching registration. Figure 6.5(B) shows the obtained registration. Figure 6.5(C) shows the registration with a sparserC view.

The above examples demonstrate that our proposed algorithm is effective for computing large deformation diffeomorphic registrations. The proposed algorithm works even with large number of landmarks or large deformations.

Figure 6.6 shows the L^2-norm of the conformality distortion (or the conformality distortion energy) versus iterations. (A), (B), (C) and (D) show the conformality distortion energy vesus iterations for the "one point landmark", "rotate sphere", "wave-shape deformation" and "twist deformation" examples respectively. Note that the conformality distortion decreases as iteration increases.

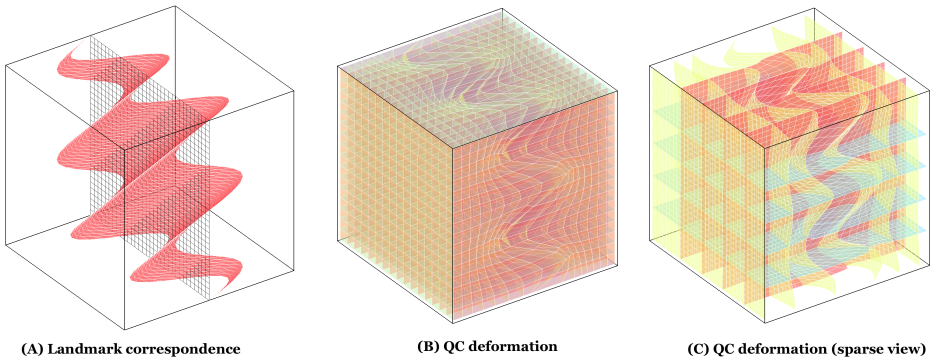

FIG. 6.4. *Constrained landmark registration with all the points on a plane are chosen as landmarks. Landmarks are deformed to a wave-shape surface. (A) shows the landmark correspondence of one point. (B) shows the obtained constrained QC registration, which is visualized as the deformed grid from the standard grid in Figure 6.1 by the obtained registration. (C) shows the sparser view of the registration.*

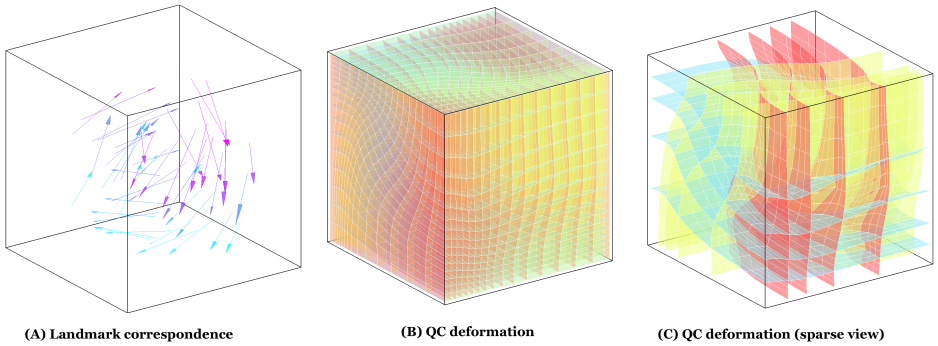

FIG. 6.5. *Constrained registration with random points being chosen as landmarks. These random landmark points are twisted. (A) shows the landmark correspondence of one point. (B) shows the obtained constrained QC registration, which is visualized as the deformed grid from the standard grid in Figure 6.1 by the obtained registration. (C) shows the sparser view of the registration.*

7. Conclusion. This paper present a new method to obtain diffeomorphic registration between general n-dimensional manifolds under very large deformations. The basic idea is to extend the 2-dimensional quasi-conformal theories to general n-dimensional spaces. Given a set of landmark constraints, our goal is to look for an optimal diffeomorphism that matches landmarks. In this paper, we introduce a notion of conformality distortion of a diffeomorphism of the n-dimensional Euclidean space. The conformality distortion measures the distortion of an infinitestimal ball to an infinitestimal ellipsoid under the diffeomorphism. Our registration problem can then be modeled as a minimization problem of an energy functional involving the conformality term and a smoothness term. The conformality term allows the algorithm to produce diffeomorphic registration even with very large deformations. Alternating direction method of multipliers (ADMM) is applied in this paper to solve the optimization problem. The algorithm only involves solving an elliptic problem and a point-wise minimization problem. The time complexity and robustness of the algorithm is independent of the number of landmark constraints. Either Dirichlet or free

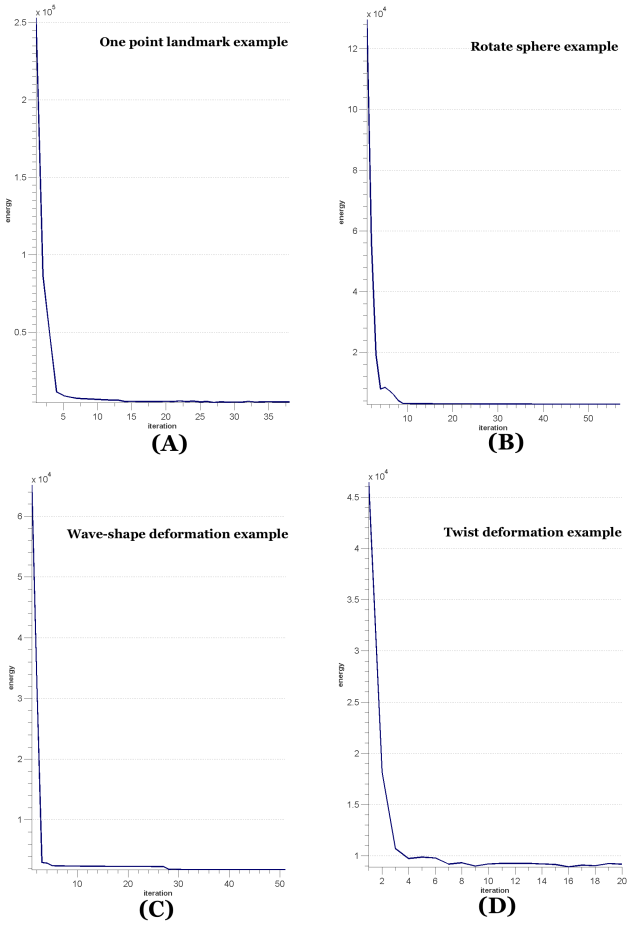

FIG. 6.6. *The L^2-norm of the conformality distortion versus iterations. (A), (B), (C) and (D) show the conformality distortion energy vesus iterations for the "one point landmark", "rotate sphere", "wave-shape deformation" and "twise deformation" examples respectively.*

boundary condition can be enforced, depending on applications. To further speed up the algorithm, the multi-grid method is applied. Experimental results show that our proposed algorithm is effective for computing large deformation diffeomorphic registrations, even with large number of landmarks or large deformations. In the future, we will test the algorithm on real medical data, such as 3D MRI scan with DTI fibre tracks as the interior landmark constraints.

REFERENCES

[1] B. Zitova and J. Flusser, *Image registration methods: a survey*, Image and Vision Computing, Volume 21, 977-1000, 2003

[2] O. Lyttelton, M. Boucher, S. Robbins, and A. Evans, *An unbiased iterative group registration template for cortical surface analysis*, NeuroImage, Vol 34, 1535-1544, 2007.

[3] J.P. Thirion, *Image matching as a diffusion process an analogy with Maxwells demons*, Medical Image Analysis, Vol 15, 112-115, 1996.

[4] B. Fischl, M. Sereno, R. Tootell, and A. Dale. High-resolution intersubject averaging and a

coordinate system for the cortical surface. *Human Brain Mapping*, 8, 272-284, 1999.

[5] X. Gu, Y. Wang, T. F. Chan, P. M. Thompson, and S.-T. Yau. *Genus zero surface conformal mapping and its application to brain*, surface mapping. IEEE Transactions on Medical Imaging, 23(8), 949-958, 2004.

[6] Y. Wang, L. M. Lui, X. Gu, K. M. Hayashi, T. F. Chan, A. W. Toga, P. M. Thompson, and S.-T. Yau. Brain surface conformal parameterization using riemann surface structure. *IEEE Transactions on Medical Imaging*, 26(6), 853-865, 2007.

[7] X. Gu and S. Yau. *Computing conformal structures of surfaces*, Communication in Information System, 2(2), 121-146, 2002.

[8] S. Joshi and M. Miller. Landmark matching via large deformation diffeomorphisms. *IEEE Transactions on Image Processing*, 9(8), 1357-1370, 2000.

[9] J. Glaunès, M. Vaillant and M. I. Miller, *Landmark Matching via Large Deformation Diffeomorphisms on the Sphere*, Journal of Mathematical Imaging and Vision, 20, 179-200, 2004.

[10] J. Glaunes, L. Younes and A. Trouve, *Diffeomorphic matching of distributions: A new approach for unlabelled point-sets and sub-manifolds matching*, IEEE Computer Society Conference on Computer Vision and Pattern Recognition (CVPR'04), 2, 712–718, 2004.

[11] J. Glaunes, A. Qiu, M. Miller and L. Younes, *Large Deformation Diffeomorphic Metric Curve Mapping*, International Journal of Computer vision, 80(3), 317-336, 2008.

[12] J. Glaunes, A. Qiu, M. Miller and L. Younes, *Surface Matching via Currents*, Proceedings of Information Processing in Medical Imaging (IPMI'05), Vol. 3565, 381-392, 2005.

[13] S. Haker, S. Angenent, A. Tannenbaum, R. Kikinis, G. Sapiro, and M. Halle. *Conformal surface parameterization for texture mapping*, IEEE Transaction of Visualization and Computer Graphics, 6, 181-189, 2000.

[14] M. K. Hurdal and K. Stephenson. *Discrete conformal methods for cortical brain flattening*, Neuroimage, 45, 86-98, 2009.

[15] M. Jin, J. Kim, F. Luo and X. Gu. *Discrete surface Ricci flow.*. IEEE Transaction on Visualization and Computer Graphics, 14(5), 1030-1043, 2008

[16] Y.L. Yang, J. Kim, F. Luo, S. Hu, X.F. Gu *Optimal Surface Parameterization Using Inverse Curvature Map*. IEEE Transactions on Visualization and Computer Graphics , 14(5), 1054-1066, 2008.

[17] W. Zeng, L.M. Lui, L. Shi, D. Wang, W.C. Chu, J.C. Cheng, J. Hua, S.T. Yau, X.F. Gu. *Shape Analysis of Vestibular Systems in Adolescent Idiopathic Scoliosis Using Geodesic Spectra.* Medica Image Computing and Computer Assisted Intervation 13(3), 538-546, 2010.

[18] L.M. Lui, T.W. Wong, W. Zeng, X.F. Gu, P.M. Thompson, T.F. Chan and S.T. Yau. *Optimization of Surface Registrations Using Beltrami Holomorphic Flow*, Journal of Scientific Computing, 50(3), 557-585, 2012

[19] L.M. Lui, T.W. Wong, X.F. Gu, P.M. Thompson, T.F. Chan and S.T. Yau. *Hippocampal Shape Registration using Beltrami Holomorphic flow*, Medical Image Computing and Computer Assisted Intervention(MICCAI), Part II, LNCS 6362, 323-330 (2010)

[20] W. Zeng, L.M. Lui, F. Luo, T.F. Chan, S.T. Yau, X.F. Gu *Computing quasiconformal maps using an auxiliary metric and discrete curvature flow.* Numerische Mathematik, 121(4), 671-703, 2012

[21] L.M. Lui, K.C. Lam, T.W. Wong, X.F. Gu *Texture Map and Video Compression Using Beltrami Representation. SIAM Journal on Imaging Science*, 6(4), 18801902, 2013

[22] T. Lin, C.L. Guyader, I. Dinov, P. Thompson, A. Toga, L. Vese *Gene Expression Data to Mouse Atlas Registration Using a Nonlinear Elasticity Smoother and Landmark Points Constraints.* Journal of Scientific Computing, 50(3), 586-609, 2012.

[23] N.A. Lord, J. Ho, B.C. Vemuri and S. Eisenschenk. *Simultaneous Registration and Parcellation of Bilateral Hippocampal Surface Pairs for Local Asymmetry Quantification*, IEEE Transactions on Medical Imaging, 26(4), 471478, 2007.

[24] T. Vercauteren, X. Pennec, A. Perchant and N. Ayache. *Diffeomorphic demons: Efficient non-parametric image registration.*, NeuroImage, 45(1), S61S72, 2009.

[25] B.T. Yeo, M.R. Sabuncu, T. Vercauteren, N. Ayache, B. Fischl, P. Golland. *Spherical demons: fast diffeomorphic landmark-free surface registration.*, IEEE Transactions on Medical Imaging, 29(3), 650668, 2010.

[26] F.L. Bookstein. *Principal Warps: Thin-Plate splines and the decomposition of deformations.*, IEEE Transactions on Pattern Analysis and Machine Intelligence, 11(6), 567-585, 1989.

[27] Y. Wang, L. Lui, T. Chan, and P. Thompson. Optimization of brain conformal mapping with landmarks. *Proceeding in Medical Image Computing and Computer-Assisted Internvention - MICCAI 2005*, 675-683, 2005.

[28] L. Lui, S. Thiruvenkadam, Y. Wang, T. Chan, and P. Thompson. *Optimized conformal param-*

eterization of cortical surfaces using shape based matching of landmark curves, Proceeding in Medical Image Computing and Computer-Assisted Internvention - MICCAI 2005, 494-502, 2008.

[29] L. Lui, S. Thiruvenkadam, Y. Wang, P. Thompson, and T. Chan. *Optimized conformal surface registration with shape-based landmark matching*, SIAM Journal of Imaging Sciences, 3(1), 52-78, 2010.

[30] L. Lui, Y. Wang, T. Chan, and P. Thompson. *Landmark constrained genus zero surface conformal mapping and its application to brain mapping research*, Applied Numerical Mathematics, 57, 847-858, 2007.

[31] D. Tosun, M. Rettmann and J. Prince. *Mapping techniques for aligning sulci across multiple brains.* Medical Image Analysis, 8, 295309, 2004

[32] F. Gardiner and N. Lakic. *Quasiconformal Teichmuller Theory.* American Mathematics Society, 2000.

[33] O. Lehto and K. Virtanen. *Quasiconformal Mappings in the Plane.* Springer-Verlag, New York, 1973.

[34] W. Zeng and X. Gu. *Registration for 3D Surfaces with Large Deformations Using Quasi-Conformal Curvature Flow.* IEEE Conference on Computer Vision and Pattern Recognition (CVPR11), Jun 20-25, 2011, Colorado Springs, Colorado, USA.

[35] X. Huang, Y. Sun, D. Metaxas, F. Sauer and C. Xu, *Hybrid Image Registration based on Configural Matching of Scale-Invariant Salient Region Features*, Proceedings of the 2004 Conference on Computer Vision and Pattern Recognition Workshop (CVPRW'04), Volume 11, 167-174, 2004

[36] D. Paquin, D. Levy and L. Xing, *Hybrid multiscale landmark and deformable image registration*, Math Biosci Eng., 4(4), 711-737, 2007

[37] T. Chanwimaluang and G. Fan, *Hybrid retinal image registration.*, IEEE Transaction on Information Technology in Biomedicine, 10(1), 129-142, 2006

[38] H.J. Johnson and G.E. Christensen, *Consistent landmark and intensity-based image registration*, IEEE Transactions on Medical Imaging, 21, 450-461, 2002

[39] H. Wang, L. Dong, J. O'Daniel, R. Mohan, A.S. Garden, K.K. Ang, and R. Cheung, *Validation of an accelerated'demons' algorithm for deformable image registration in radiation therapy*, Physics in Medicine and Biology, 50(12): 2887, 2005

[40] B. Glocker, N. Komodakis, N. Paragios and N. Navab *Approximated curvature penalty in non-rigid registration using pairwise mrfs*, 5th International Symposium on Visual Computing (ISVC), Las Vegas, Nevada, USA, November 2009

[41] B. Glocker, N. Komodakis, N. Paragios, G. Tziritas, and N. Navab *Inter and intra-modal deformable registration: Continuous deformations meet efficient optimal linear programming*, Information Processing in Medical Imaging, Kerkrade, Netherlands, July 2007.

[42] B. Glocker, N. Komodakis, G. Tziritas, N. Navab, and N. Paragios *Dense image registration through mrfs and efficient linear programming*, Medical Image Analysis, 12(6):731741, 2008.

[43] B. Glocker, A. Sotiras, N. Komodakis and N. Paragios *Deformable Medical Image Registration: Setting the State of the Art with Discrete Methods*, Annual Review of Biomedical Engineering, 12(12), 219-244, 2011